Received: 18 December 2020 | Revised: 25 May 2021 | Accepted: 28 May 2021

DOI: 10.1002/joc.7228

RESEARCH ARTICLE

International Journal of Climatology RMetS

The Swiss Alpine zero degree line: Methods, past evolution and sensitivities

Simon C. Scherrer[1] | **Stefanie Gubler**[1] | **Kathrin Wehrli**[1,2] | **Andreas M. Fischer**[1] | **Sven Kotlarski**[1]

[1]Federal Office of Meteorology and Climatology MeteoSwiss, Zurich-Airport, Switzerland

[2]Center for Climate Systems Modeling C2SM, ETH, Zürich, Switzerland

Correspondence
Simon C. Scherrer, Federal Office of Meteorology and Climatology MeteoSwiss, Operation Center 1, Post box, CH-8058 Zurich-Airport, Switzerland.
Email: simon.scherrer@meteoswiss.ch

Abstract

The near-surface zero degree line (ZDL) is a key isotherm in mountain regions worldwide, but a detailed analysis of methods for the ZDL determination, their properties and applicability in a changing climate is missing. We here test different approaches to determine the near-surface ZDL on a monthly scale in the Swiss Alps. A non-linear profile yields more robust and more realistic ZDLs than a linear profile throughout the year and especially in the winter-half year when frequent inversions disqualify a linear assumption. In the period 1871–2019, the Swiss ZDL has risen significantly in every calendar month: In northern Switzerland, the monthly ZDL increases generally amount to 300–400 m with smaller values in April and September (200–250 m) and a larger value in October (almost 500 m). The largest increases of 600–700 m but also very large uncertainties (±400 m, 95% confidence interval) are found in December and January. The increases have accelerated in the last decades, especially in spring and summer. The ZDL is currently increasing by about 160 m·°C^{-1} warming in the summer-half year and by up to 340 ± 45 m·°C^{-1} warming in winter months. In southern Switzerland, ZDL trends and temperature scalings are somewhat smaller, especially in winter. Sensitivity analyses using a simple shift of the non-linear temperature profile suggest that the winter ZDL-temperature scalings are at a record high today or will reach it in the near future, and are expected to decrease with a strong future warming. Nevertheless, the cumulative ZDL increase for strong warming is considerably larger in winter than in summer. Based on a few key criteria, we also present best practises to determine the ZDL in mountain regions worldwide. The outlined methods lay a foundation for the analysis of further isotherms and to study the future ZDL evolution based on climate scenario data.

KEYWORDS

Alps, climate change, isotherms, mountains, non-linearities, Switzerland, trends, zero degree line

This is an open access article under the terms of the Creative Commons Attribution License, which permits use, distribution and reproduction in any medium, provided the original work is properly cited.
© 2021 The Authors. *International Journal of Climatology* published by John Wiley & Sons Ltd on behalf of Royal Meteorological Society.

1 | INTRODUCTION

Atmospheric isotherms, that is, lines of equal or constant air temperature, are a central concept in climatology. Their near-surface patterns are used in climate classification and climate zoning (Kottek *et al*., 2010; Rubel *et al*., 2017) and inform, for instance, the spatial and vertical distribution of ecosystems and cryospheric features. In mountainous terrain, the vertical distribution of near-surface isotherms is ultimately related to the near-surface temperature lapse rate, the major source of spatial temperature variability (Lute and Abatzoglou, 2021). It controls the spatial extent of temperature zones and thereby (co-)determines the variation of temperature-dependent land surface features (vegetation, soil type) and anthropogenic structures (settlements, agricultural land, etc.) on comparatively small horizontal distances. The vertical distribution of isotherms in the free atmosphere, on the other hand, controls the thermodynamic state, atmospheric stability, large-scale dynamics and both regional and global scale feedback mechanisms (Bony *et al*., 2006; Kröner *et al*., 2017; Brogli *et al*., 2019). With temperature changes being a primary indicator of global climate change, shifts in the location and three-dimensional structure of isotherms have been observed in the past (Diaz and Graham, 1996; Diaz *et al*., 2003; Carrasco *et al*., 2005) and are also to be expected under future climate change (Beniston, 2014; Kotlarski *et al*., 2015).

While the general concept of isotherms has a large range of applications, a special isotherm is of particularly high relevance and is frequently employed in the existing literature: the zero degree line (ZDL; also referred to as *0°C line* or *0°C isotherm*, in the free-atmosphere case also as *freezing level [FL]* or *freezing height*; Bradley *et al*., 2009). In two-dimensional space it is defined as the line connecting locations of 0°C air temperature and can also be extended to a three-dimensional zero degree surface or, for a given location or region, as an elevation of the ZDL/zero degree surface above sea level. In the following, we will refer to this elevation as the ZDL. In mountain regions, the ZDL roughly separates regions where precipitation predominantly falls as snow or as rain (Hock *et al*., 2019) and is connected to both the snowline (Diaz *et al*., 2003; Ceppi *et al*., 2012; Hüsler *et al*., 2014) and the equilibrium line of glaciers (Carrasco *et al*., 2005) and, ultimately, to discharge in glaciated and/or snow-dominated catchments (Immerzeel *et al*., 2014).

Despite the relevance of the ZDL in mountainous regions, only few studies have so far investigated its spatial variability, its long-term changes and its sensitivity to regional climate change. Existing works are often related to the analysis of temperature lapse rates for example, in the Andes (Carrasco *et al*., 2005; Bradley *et al*., 2009; Schauwecker *et al*., 2017; Ibañez *et al*., 2020), the Himalayas (Kattel *et al*., 2013), the Cascade Mountains (Minder *et al*., 2010), the Carpathian mountains (Micu *et al*., 2020) and the European Alps (Rolland, 2003; Kirchner *et al*., 2013; Hiebl and Schöner, 2018). For the latter case, the recent CH2018 Climate Scenarios for Switzerland found an increasing ZDL under future climate change with uplift rates depending on the specific greenhouse gas scenario considered (CH2018, 2018). Past changes of the regional ZDL are also regularly communicated via annual climate reports (e.g., MeteoSchweiz, 2019). In many cases, a straightforward comparison of existing works and their respective results is difficult as there is no single and widely accepted methodology to derive the ZDL. This is partly connected to the diversity of intended applications. In principle, the ZDL can be derived either from upper air data (radio soundings or vertical levels of atmospheric models; Bradley *et al*., 2009, Brocard *et al*., 2013, Diaz *et al*., 2003 and Güller, 1979) or from near-surface temperatures observed or simulated at different locations (Lüthi *et al*., 2019; Dutra *et al*., 2020). In the former case, the ZDL represents a characteristic of the atmospheric column which is controlled by synoptics but which can also include imprints of surface–atmosphere exchange processes. It is relevant for stability considerations and cloud microphysics (Pruppacher and Klett, 2010; Korolev *et al*., 2017). In the latter case, the derived near-surface ZDL represents a quantity that is considerably influenced by processes within the planetary boundary layer and at the surface–atmosphere interface. It has a high relevance for surface-based applications such as those related to the terrestrial cryosphere or plant ecology. Besides these differences in the nature of the underlying temperature data, the ZDL can be derived employing different methodological approaches which can yield different ZDL estimates (see Section 2 for more details). Common to all approaches are problems due to (a) near-surface or elevated inversions, that is, strong nonlinearities of the vertical temperature profile that could for instance lead to the existence of several ZDLs above a given point of interest and (b) an actual ZDL that is lower/higher than the minimum/maximum elevation of all considered temperature measurements and the necessity to extrapolate the vertical temperature profile into the non-sampled elevation space or even below the surface.

The present work is devoted to shed more light on this unsatisfactory situation, to compare and evaluate existing approaches for deriving the ZDL with the ultimate goal to enable a climatological analysis of the temporal ZDL evolution in a climate change context. In general, a decent understanding of the past evolution of the ZDL in a given region of interest is important to set the generally expected future rise of the ZDL into a historic context. We choose Switzerland as a testbed that is subject to important orographic variability and that features high-quality and long-term observational series of air temperature covering a large elevational range. We

focus on a regional near-surface ZDL as derived from near-surface monthly temperature data. These are available in many other regions which, potentially, enables a transferability of our approach. The specific research questions to be answered are as follows:

- How did the Swiss Alpine ZDL evolve in the last 150+ years and what is the sensitivity of the regional ZDL to large-scale warming?
- What are the advantages and disadvantages of different methodologies to derive a regional ZDL in a climate change context?
- Can we provide best practises for a regional ZDL determination and the analysis of long term ZDL changes?

Answering these questions will inform and facilitate the analysis of future projections of the ZDL, which is planned to be carried out in a follow-up work.

2 | DATA AND METHODS

2.1 | Study region

Our testbed is Switzerland, a country located in Central Europe, with highly complex topography and an area of approximately 41,300 km^2 (Figure 1). About 60% of the country's area belongs to the European Alps, a 'croissant-shaped', predominantly west–east elongated mountain range (west–east extension: ~800 km, north–south extension: ~200 km) with high peaks (>4,000 m asl) and deep valleys (valley floor elevations often <1,000 m asl). Most of the Swiss Alpine domain is located north of the main divide of the Alps (northern Switzerland below). The northern foreland area, a hilly region called Swiss Plateau with elevations between 300 and 900 m asl where most of the Swiss population lives, covers 30% of the Swiss area. Further about 10% of the Swiss area belong to the Jura mountains, a mountain range with elevations up to 1,600 m asl, located west and north-west of the Plateau. The topographic situation with the Swiss Plateau as partially enclosed basin between the Jura mountains and the Alps creates a climate with frequent cold-air pooling, fog situations and temperature inversions in the winter-half year (Wanner and Kunz, 1983; Scherrer and Appenzeller, 2014; Salzmann *et al*., 2015). Only small parts of Switzerland (<10%) are located south of the main divide of the Alps (southern Switzerland below). The region has a milder climate and is largely influenced by Mediterranean air masses (Schär *et al*., 1998; Scherrer, 2006). We therefore compute and discuss the ZDLs for northern and southern Switzerland separately.

2.2 | Data

High-quality station data is available in Switzerland for more than 150 years. The measurement locations used

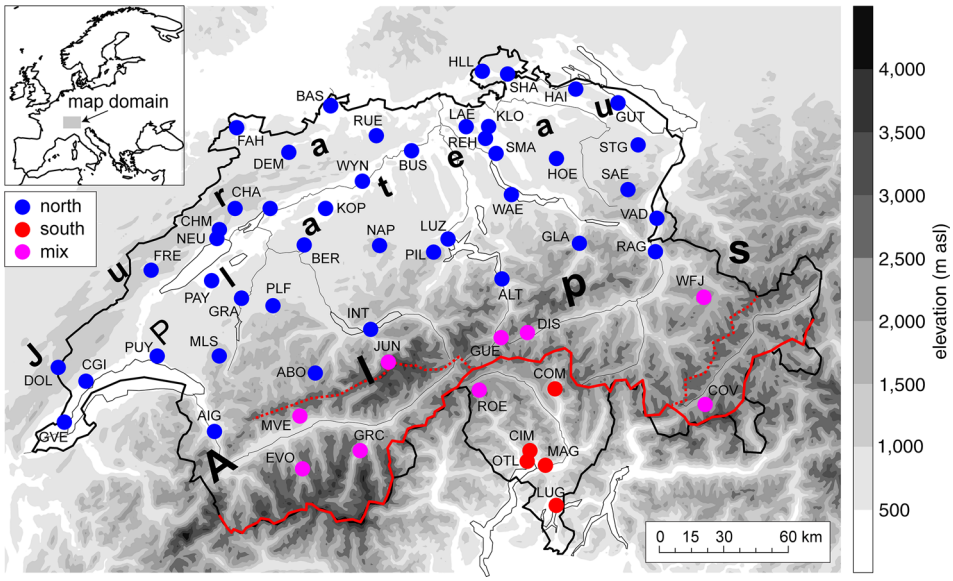

FIGURE 1 Map of Switzerland and 57 locations used in this study. Locations solely used to construct the northern (southern) Swiss profiles are shown in blue (red). Locations used in both profiles are shown in pink. Abbreviations and weighting details are given in Table S1. The grey shading shows the orography in metres above sea level. The solid red line shows the course of the main Alpine divide, the dashed red lines show further main topographic divides. The three main regions, Jura (~10% of Swiss area), Plateau (~30% of Swiss area) and Alps (~60% of Swiss area), are marked by lettering. The inset in the top left shows the location of the map domain within Europe (grey area) [Colour figure can be viewed at wileyonlinelibrary.com]

for this study cover a large elevation range from 205 to 3,574 m asl (Table S1). The elevation range of the historic monthly ZDL is quite well sampled by the station data. Switzerland is thus one of the few places where the long-term evolution of a regional near-surface ZDL can be studied in great detail. Specifically, we use the monthly gridded Isotta *et al.* (2019) temperature data set that covers the years 1864–2019. It merges spatial information from high-resolution gridded data sets based on a relatively dense network (60+ stations) over a limited time period (1961-today) with long-term information from individual homogeneous and fully continuous station series. It delivers temporally consistent monthly temperature information on a Switzerland-wide 2.2 km grid and provides a better data basis than station data with only about 20 stations with very long and continuous data series. The typical error of the gridded data set is about 0.2°C on the monthly time scale. In this study, only a small subset of grid points will be used for the ZDL estimation (Section 2.3.2). To assess the performance of the gridded data set we additionally use daily and monthly station data from 57 MeteoSwiss stations (Table S1/Figure 1). Note that except for validation purposes (Section 3), the near-surface ZDL is derived from monthly mean temperature data.

As a complementary data set and for comparison purposes, the freezing level (FL) in the free atmosphere from the only radiosonde in Switzerland is used. The sondes are launched in Payerne located on the Swiss Plateau and the data is available twice a day (at 00 and 12 UTC). The FL is determined from these radio soundings using the method described in Güller (1979). As in other studies (Lynn *et al.*, 2020), the FL with the highest elevation is used. If the FL is below the surface, the temperatures are extrapolated with a lapse rate of −0.5°C per 100 m until the FL is reached. Daily FL values are computed as the mean of the 00 and 12 UTC values, monthly values are computed as the mean of all available 00 and 12 UTC values. Currently, reliable data is available since 1954, hence the period used covers the years 1954–2019.

2.3 | Regional near-surface ZDL

2.3.1 | General approaches

The near-surface ZDL can vary considerably in space, especially in regions with cold-air pooling like northern Switzerland in winter. It is thus not straightforward to determine a high-resolution ZDL field for a long-term analysis. Here, we determine regional estimates. Two general concepts are conceivable to determine a regional near-surface ZDL. The first concept is non-parametric and purely data driven. It is based on a simple averaging of station (or grid-point) elevations where temperatures are close to 0°C (*near 0°C* below). The second concept is to fit a parametric temperature (T) profile with respect to elevation (z). A large number of parametric functions is conceivable. In this article, we discuss two parametric T–z profiles: a linear T–z profile (*linear fit* below) and a non-linear T–z profile (*non-linear fit* below). The ZDL is derived as the elevation z where $T(z) = 0$°C.

Figure 2 schematically illustrates how the ZDL is determined using the *near 0°C*, *linear fit* and *non-linear fit* methods for an almost linear profile (Figure 2a) and for a highly non-linear profile with a strong temperature inversion (Figure 2b). The corresponding ZDL estimates can strongly differ, especially if the temperature profile is highly non-linear for temperatures close to 0°C. However, also in nearly linear situations, the ZDL estimates can differ considerably, especially if the ZDL is at the edge or even outside the elevation range covered by the observations. In addition, the *non-linear fit* and *near 0°C* method allow several ZDLs. This illustration indicates that an in-depth investigation of the regional conditions, data and methodological requirements, as well as key properties of the three approaches is needed to come up with best practises for the ZDL determination.

2.3.2 | Approaches for the Swiss Alps

The *near 0°C* method does not work if the ZDL is outside the elevation range covered by the data. Although the ZDL in the Swiss Alps is often within the elevation range covered by observations, extrapolation below the surface is necessary in cold months and potentially above the highest peaks in a warmer future. Therefore, we compare the monthly T–z profiles and the ZDL derived from them specifying the two parametric T–z profiles introduced above as follows:

1. A linear T–z profile (*linear* profile below) is implemented as ordinary least squares linear regression of temperature with respect to elevation. This profile is most commonly used in environmental studies (Rolland, 2003; Blandford *et al.*, 2008; Lute and Abatzoglou, 2021). It delivers a constant lapse rate γ, defined as the slope of the linear function over the whole elevation range, and a unique ZDL (*linear* ZDL below).
2. A non-linear T–z profile (*inv_type* profile below) is implemented employing the non-linear parametric profile introduced by Frei (2014), originally developed for daily temperature profiles. It allows a flexible

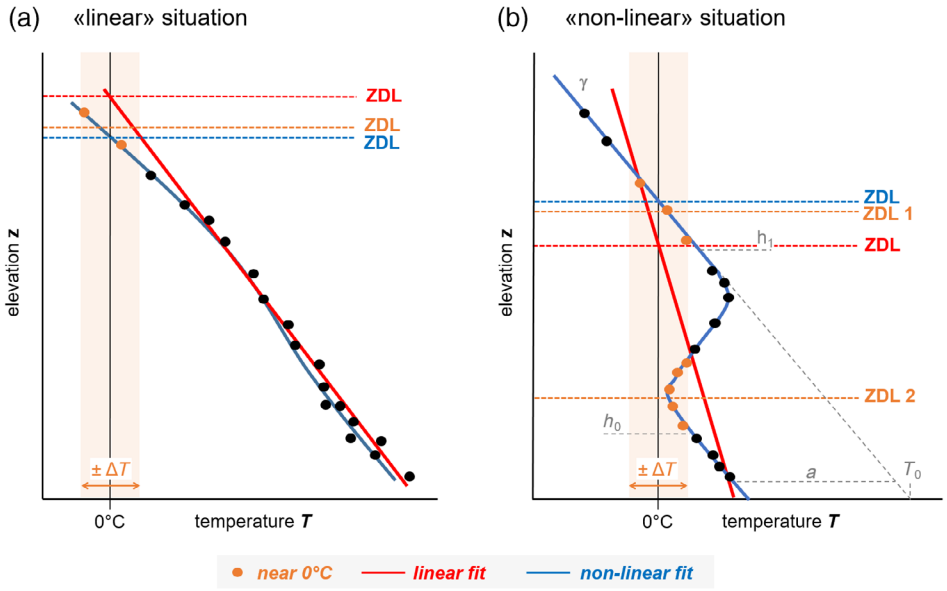

FIGURE 2 Schematic example of the ZDL determination using the *near 0°C*, *linear fit* and *non-linear fit* methods for a relatively linear situation (Panel a, left) and a highly non-linear inversion situation (Panel b, right). Shown are temperature profiles (temperature T vs. elevation z) with measurements (points), the fits (*linear fit* in red, *non-linear-fit* in blue) and the *near 0°C* band ($\pm\Delta T$) and used data points in orange. The dashed lines show the ZDLs determined with the three different methods. In Panel b, the five parameters (h_0, h_1, γ, T_0, a) of the non-linear profile applied in this article are shown [Colour figure can be viewed at wileyonlinelibrary.com]

modelling of different common non-linearities including inversions as follows:

$$T(z)=\begin{cases} T_0-\gamma z & z\geq h_1 \\ T_0-\gamma z-\dfrac{a}{2}\left(1+\cos\left(\pi\cdot\dfrac{z-h_0}{h_1-h_0}\right)\right) & h_0<z<h_1 \\ T_0-\gamma z-a & z\leq h_0 \end{cases}$$

The profile has two linear sections, one at upper levels (above h_1) and one at lower levels (below h_0), both sharing the same lapse rate γ. T_0 denotes the intercept (temperature at elevation $z = 0$) of the upper linear section. The two linear sections are shifted against each other by a temperature contrast a and are connected in the intermediate elevation range by a smooth step function (using cosines), imitating an inversion layer. The five profile parameters are estimated all together using weighted non-linear least squares without supervision. Methodological details including information of how to choose a good set of initial values for the profile parameters for the optimization procedure are available in Frei (2014) on page 1590. Figure 2b illustrates the profile parameters. Note that, the profile can become linear if a is zero. The method delivers one to three ZDLs (*inv_type* ZDL below) which are computed using bilinear interpolation between the 25 m elevation steps of the discrete fit. For the analysis, as for the FL above, the highest ZDL is chosen. See Section 3.2 for an additional validation based justification of this choice.

To construct the *linear* and *inv_type* profiles as basis for the ZDL determination, 57 locations have been considered (Ffigure 1, Table S1). We use the same locations as Frei (2014). The selection was mainly guided by the regional representativity of the local physiographic characteristics but also data availability and homogeneity. Locations strongly influenced by very local cold-pools (i.e., with a comparatively large mean daily temperature range) have been omitted. The location data were weighted according to their representativeness for northern and southern Switzerland using geographical position (Table S1 for the individual weights for the northern and southern T–z profile). In total 52 locations are used to estimate the northern Swiss profile (blue/pink points in Figure 1) and 14 locations for the southern Swiss profile (red/pink points in Figure 1). As explained in Section 2.2, the temperature data at each individual location is not obtained from the actual station series but from the grid point of the Isotta *et al.* (2019) data set with the smallest elevation difference to the station elevation checking the closest and the eight directly surrounding grid points. The use of grid point temperatures yields very similar ZDL estimates as the use of actual station data in the 1990–2019 validation period (cf., Section 3.2).

3 | VALIDATION AND CHOICE OF METHOD

In this section, we evaluate the properties of the *linear* and *inv_type* profiles and the resulting ZDLs constructed using monthly mean temperature data and select the preferred approach for the analysis of the Swiss Alpine ZDL climatology. We start with a discussion of the profile properties and errors (Section 3.1). We then examine consequences of biased temperature profiles and additional complicating factors on the ZDL estimates (Section 3.2) and compare the ZDL estimates with the FL (Section 3.3). In Section 3.4, the properties are summarized and the preferred method is chosen.

3.1 | Temperature profiles

Figure 3 shows the averaged monthly temperature profiles for the 30-year norm period 1981–2010. The autumn and especially the winter curves of the *linear* profiles are much steeper (show smaller lapse rates) than their spring and summer counterparts (Figure 3a,b). At high elevations, this leads to large differences compared to the *inv_type* profiles (Figure 3c,d). The *inv_type* profiles depict considerable non-linearities even in the 30-year means shown here. Non-linearities are considerable around 0°C in late autumn and winter at elevations between 500 and almost 2,000 m asl, which marks the well-known winter-half year inversion tops over northern Switzerland (Scherrer and Appenzeller, 2014).

Figure 4 shows the smoothed mean profile errors as a function of elevation for the whole historical period 1864–2019. The *linear* profile errors for northern Switzerland (Figure 4a) range from −0.8 to almost +3°C and heavily depend on the month and elevation. They are small (<0.25°C) for elevations below 1,000 m asl. The *linear* profile underestimates temperatures at elevations between 1,000 and almost 2,500 m asl. At these elevations, the errors are largest in winter and autumn with values between −0.5 and −0.8°C and a maximum around 1,500 m asl. This elevation corresponds well with the typical inversion and high-fog top in autumn and winter (Scherrer and Appenzeller, 2014). Above 2,500 m asl, temperatures are strongly overestimated. Again, the errors are larger in autumn and winter (1–3°C at

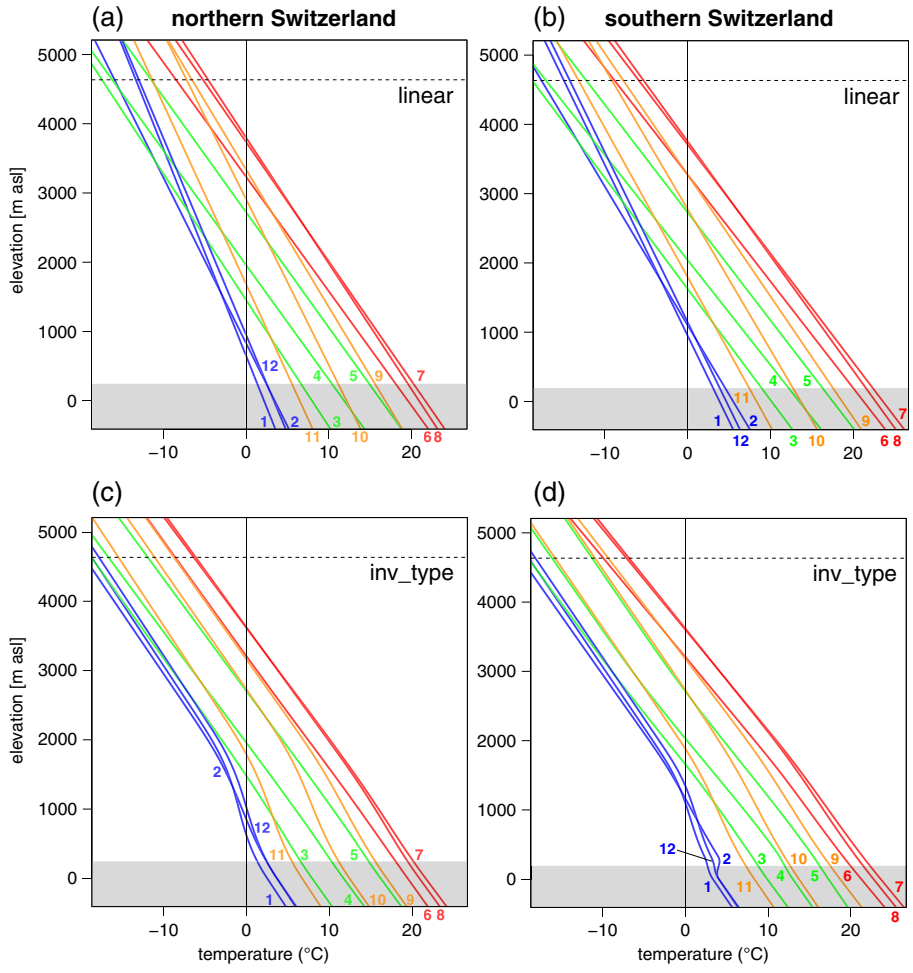

FIGURE 3 Temperature–elevation (T–z) profiles for the 1981–2010 mean for each calendar month using the *linear* profile (upper Panels a,b) and the *inv_type* profile (lower Panels c,d) for northern Switzerland (left Panels a,c) and southern Switzerland (right Panels b,d). Winter months are shown in blue (12: December, 1: January and 2: February), spring months in green (3: March, 4: April, 5: May), summer months in red (6: June, 7: July, 8: August) and autumn months in orange (9: September, 10: October, 11: November). The grey area shows elevations below the lowest topographic points in the region. The dashed line shows the highest elevation of the Swiss topography (4,634 m asl) [Colour figure can be viewed at wileyonlinelibrary.com]

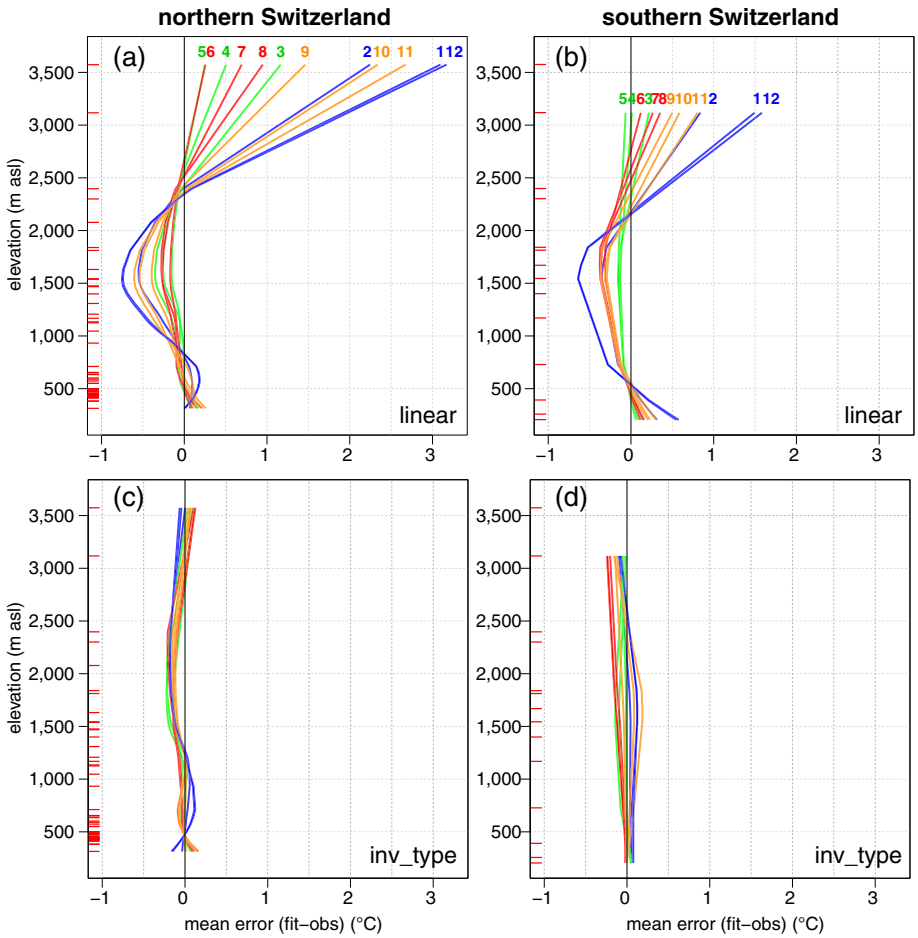

FIGURE 4 Mean monthly errors (profile fit minus station observations in °C) for the *linear* profile (upper Panels a,b) and the *inv_type* profile (lower Panels c,d) for northern Switzerland (left Panels a,c) and southern Switzerland (right Panels b,d). Time period considered is 1864–2019. The colours show the meteorological seasons (DJF: blue, MAM: green, JJA: red and SON: orange), in Panels a,b the months are also numbered. The red dashes on the left side of the panel show the elevations of the 49 (14) locations used for the profile estimations for northern (southern) Switzerland. The curves are LOESS (LOcally Estimated Scatterplot Smoothing, Cleveland *et al.*, 1992) smoothed with a smoothing parameter $f = 0.8$ ($f = 2$) for northern (southern) Switzerland [Colour figure can be viewed at wileyonlinelibrary.com]

~3,500 m asl) than in spring and summer (0.25–1°C). In contrast, the errors of the northern Swiss *inv_type* profile are very small (Figure 4c). They are smaller than 0.2°C for all elevations, indicating that the *inv_type* profile is able to mimic non-linearities excellently in all months. The general error structure for southern Switzerland is similar with slightly smaller errors for the *linear* profile (error range from −0.6 to 1.5°C, Figure 4b) and slightly larger errors for the *inv_type* profile (<0.3°C, Figure 4d).

3.2 | ZDL estimates

The elevation dependence of the *T*–*z* profile errors discussed above and the strong seasonal cycle of the ZDL complicate a translation of the profile error into a ZDL error. However, the combination of the climatological ZDL with the *T*–*z* profile errors allows some general comments of the influence of the profile errors on the ZDL. The winter months ZDL in the Swiss Alps is often between 500 and 1,500 m asl. The *T*–*z* profile errors are relatively small for elevations below 1,000 m asl but in warmer years with a ZDL well above 1,000 m asl, the *linear* profile showing negative errors tends to produce ZDL estimates that are too low. The large errors of the *linear* profile at high elevations (Figure 4a,b) are only of minor relevance for the ZDL determination in winter but they may be relevant for isotherms below 0°C. In summer and autumn on the other hand, the ZDL is often between 3,000 and 4,000 m asl. Here, the *linear* profile overestimates temperatures and the ZDL (Figure 4a,b and discussion of Figure 6, below). The problems increase with rising temperatures, as is expected in the future.

Beside the sensitivities related to errors in the representation of the *T*–*z* profile, several additional factors can potentially distort the determination and interpretation of the ZDL (see Supporting Information Section S1). We found that

- the influence of slightly smaller errors of the Isotta *et al.* (2019) data set in the 1981–2010 calibration period compared to the years before 1981 and after 2010 had no substantial effect on the ZDL and its evolution
- the ZDL determined from the monthly mean temperature profile is reasonably close to the monthly ZDL derived by averaging daily ZDL values with clearly smaller differences for the *inv_type* profile than the *linear* profile. There are some winter months with

deviations where the concept of a mean monthly ZDL has a limited applicability, but it still seems reasonable to justify a monthly approach if the limitations and the partly substantial uncertainties are properly discussed.

- the influence of using representative grid points of the Isotta *et al.* (2019) data set instead of actual station data is very small for the whole elevation range of the ZDL values in the Alps

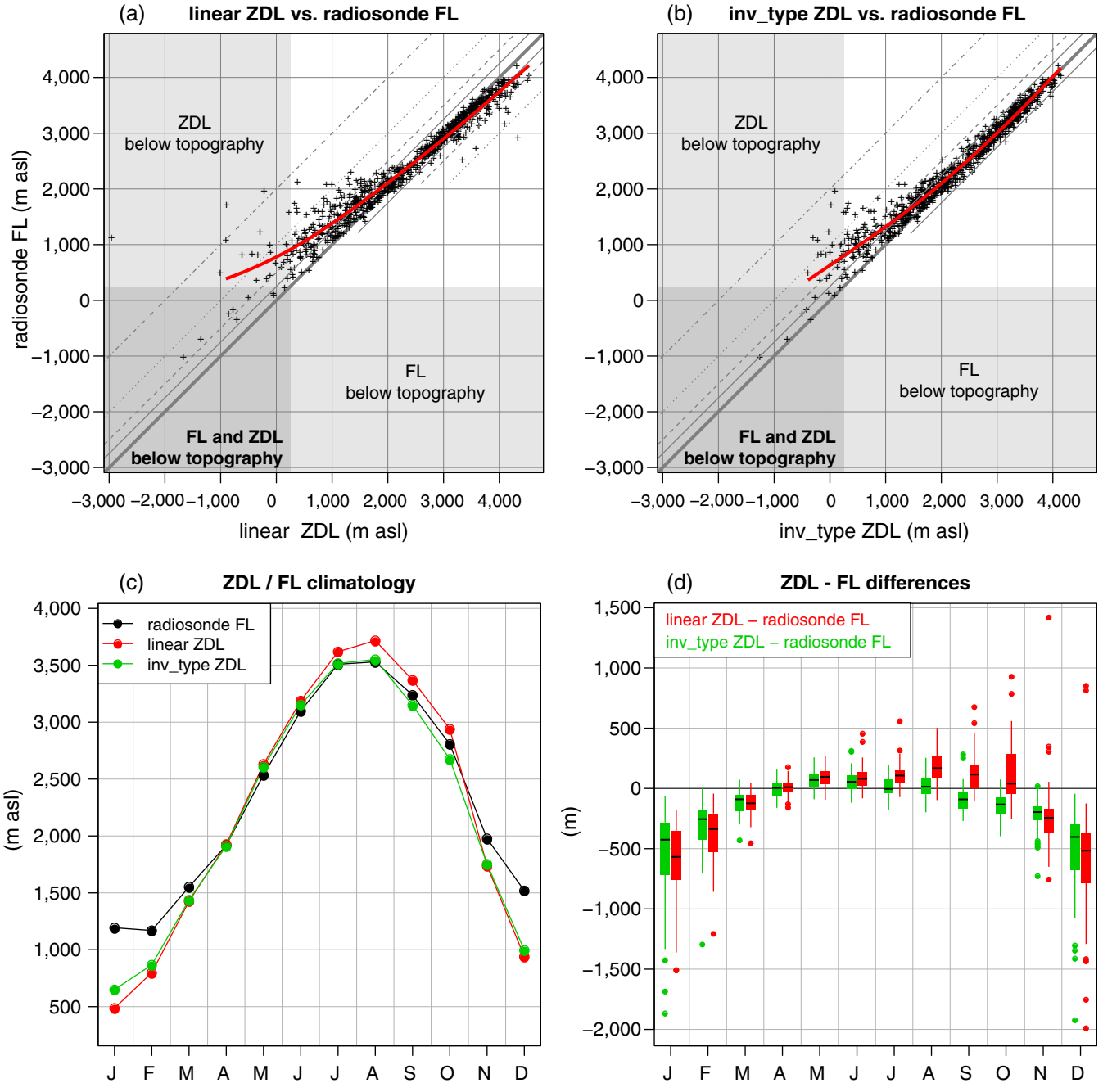

FIGURE 5 Comparison of monthly northern Swiss estimates of the FL and the highest near-surface *linear* and *inv_type* ZDL in the period 1954-2019 (n=792 months). Panel a: scatterplot of all monthly estimates (crosses) of the *linear* ZDL against the FL. Panel b: same as in panel a but for the *inv_type* ZDL. The grey lines show difference isolines (thick solid line: 0 m, solid line: ±200 m, dashed line: ±500 m, dotted line: ±1,000 m, dash-dotted line: 2,000 m). The bold red lines show a LOESS smoother (cf., Figure 4) with $f = 1$. The light (dark) grey shaded areas show the elevation ranges where the ZDL or FL (ZDL and FL) are below the topography. Panel c: climatology of mean monthly FL (black), *linear* ZDL (red) and *inv_type* ZDL (green). Panel d: boxplots of all monthly ZDL-FL differences (*linear*: red, *inv_type*: green) [Colour figure can be viewed at wileyonlinelibrary.com]

- only four (46) months of the 1872 months in the 1864–2019 period show more than one ZDL for the northern (southern) Swiss ZDL using the *inv_type* profile based on monthly profiles (cf., Figure S2). Most of the middle ZDLs and lower ZDLs lie below the topography. The highest ZDL seems the most physically meaningful time series to analyse in our setting.

3.3 | Comparison of the ZDL and the freezing level

In this section, we compare the two regional near-surface ZDL estimates with each other and with the northern Swiss free-air FL based on radiosonde data. It is well known that near-surface and free-air temperatures behave differently (Richner and Phillips, 1984; Pepin and Seidel, 2005) and as a consequence, the ZDL and FL are not the same (Brocard *et al*., 2013). Nevertheless, a comparison of ZDL and FL provides valuable information for choosing the best ZDL method.

The northern Swiss monthly *linear* ZDL (Figure 5a) deviates systematically from the free-air FL. The ZDL values above 2000 m asl are higher than the FL, on average by about 250 m, sometimes by more than 500 m. One reason is that the *linear* profile shows a strong positive bias at high elevations (Figure 4a). ZDL values below 2,000 m asl tend to be substantially lower than the FL, and the differences are larger than for the higher elevations, on average more than 400 m at 1,000 m asl, and about 700 m at the lowest point of northern Switzerland. About 20 months show differences around or larger than 1,000 m. Such large differences are found in those months during which the assumption of a linear relationship between elevation and temperature is completely inappropriate (see below). The *inv_type* ZDLs (Figure 5b) are in general closer to the FL than the ZDL of the *linear* profile and almost unbiased with respect to the FL for elevations above 2,000 m asl. The differences are mostly limited to ±200 m. For ZDLs below 2,000 m asl, the FL is typically higher, on average about 300 m higher at 1000 m asl and 500 m higher at the lowest point of northern Switzerland. For about 10 months, the differences are larger than 1,000 m. This mainly happens when a FL is detected, that is caused by an inversion at mid-elevations that just exceeds the 0°C limit, and the *inv_type* profile stays below the 0°C limit. Figure 5c shows the monthly ZDL and FL climatologies for the period 1954–2019. It confirms that the mean differences between ZDL and FL are small (±200 m) at mid-elevations (~2,000 m asl), especially in spring. In summer and parts of autumn, the *inv_type* ZDL is on average closer to the FL than the *linear* ZDL. In winter (DJF), the near-surface ZDLs are on average 300–600 m lower than the FL, which is in agreement with earlier results (Güller, 1979; Brocard *et al*., 2013). Figure 5d displays the differences between the ZDLs and the FL for the single months. In summary, the *inv_type* ZDL is closer to the FL than the *linear* ZDL in most cases. However, both near-surface ZDLs deviate considerably from the FL in winter time. Parts of these differences could be physical (e.g., cooler ground, especially when snow covered) but a quantification is beyond the scope of this article.

Figure 6 shows all ZDL differences between the *inv_type* and *linear* ZDL for the 1864–2019 period for all months of the year. The median differences are very small from March to June (around or <10 m). Negative median differences (i.e., higher *linear* ZDL) are found from July to October with a northern Swiss minimum of almost −200 m in September and a smaller southern Swiss minimum of about −120 m in August. The *linear* ZDL is higher than the *inv_type* ZDL due to the combined effect of increasing non-linearities (cold-air pooling) in late summer/early autumn and the fact that the ZDL is still at high elevations and thus not well represented by the linear fit. Positive median differences (i.e., higher *inv_type* ZDL) are found from November to February with a maximum in January (northern Switzerland) and in December (southern Switzerland). Except for December in southern Switzerland, the late autumn/winter differences are smaller than in summer/early autumn. In autumn/winter the ZDL is at lower elevations where the linear fit works better. For northern Switzerland, there are 23 months from October to February with absolute ZDL differences larger than 1,000 m while in southern Switzerland there are no cases with such large differences. The largest differences are obtained for very cold months with ZDLs well below the lowest point of the topography in combination with strong inversion signals (i.e., a highly non-linear T–z relationship, Figure S3). The *linear* T–z profile can become very steep (e.g., in January 1864, December 1871 or January 1880) or in December 1879 the slope is even positive (temperature increase with elevation). Another class of months leading to very high differences is mainly found in autumn or early winter (e.g., October 1921, 1965, 1969, November 2011, or December 2015). In these cases, the *linear* profile produces much higher ZDLs because it overestimates temperatures at high elevations.

3.4 | Choice of method

The validation of the temperature profiles, the methodological sensitivity tests, the comparison with the free-air FL, and the analysis of the cases with large differences

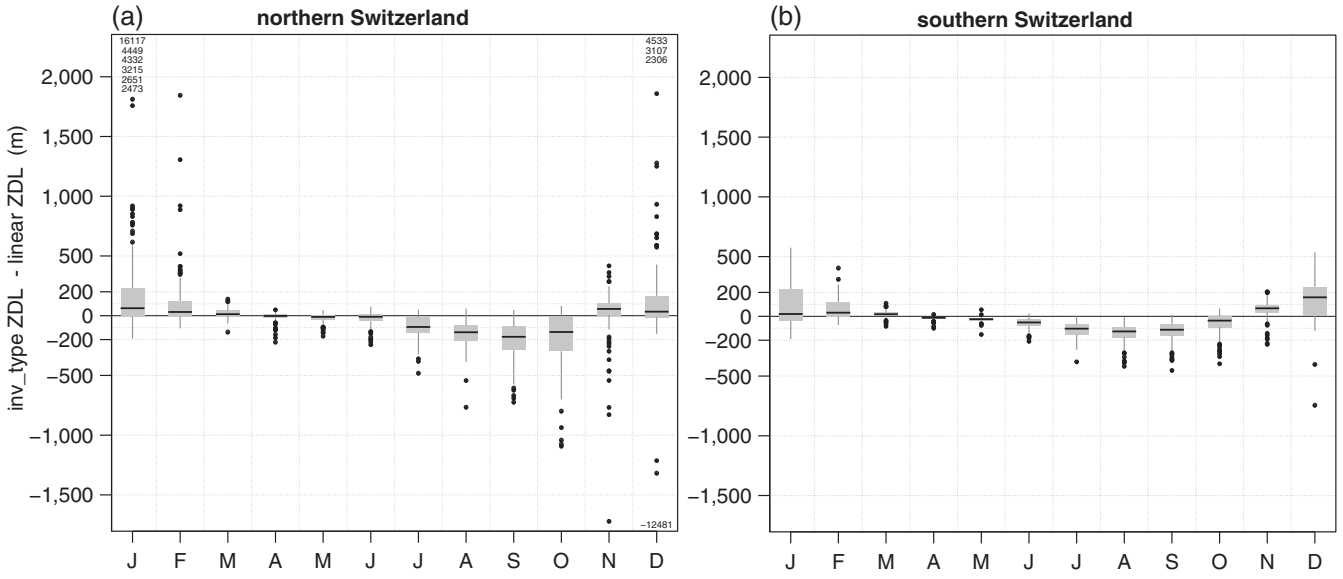

FIGURE 6 Boxplots of all 1872 monthly ZDL elevation differences (*inv_type* ZDL minus *linear* ZDL) for northern (southern) Switzerland in Panel a, b for the period 1864–2019. Note that, a few very positive and negative January and December values have been cut off. Their values are written (in m) in the plot

between the two profile methods help to choose a method for the derivation of the ZDL in the Swiss Alps. Basically all factors favour the *inv_type* profile: It is highly flexible, represents the T–z profile better than a *linear* profile and works well with both, highly non-linear and nearly linear profiles. The *inv_type* profile is also much more robust than the *linear* profile, which can show very steep or even positive slopes (increasing temperature with elevation), leading to unrealistically low or high ZDLs. The *inv_type* profile also gives more consistent results with monthly mean data when compared to monthly averaged daily ZDLs although some limitations of the ZDL concept in winter months exist. In addition, it represents the high-elevation stations much better. The *linear* profile is biased at high elevations, which can potentially become very relevant in summer with rising ZDLs in the future. Finally, the *inv_type* ZDL values are closer to the free-air FL, especially for ZDLs above 2,000 m asl and in situations where large ZDL differences are found between the *linear* and *inv_type* ZDL. In the following, we therefore exclusively use the highest *inv_type* ZDL to discuss the past Swiss ZDL climatology and sensitivity to further warming.

4 | PAST CLIMATOLOGY

4.1 | Annual cycle

As for temperature in the European Alps in general, there is a strong seasonal cycle in the ZDL (Figure 7) with the lowest values in January (values mostly between 0 and 1,000 m asl, sometimes below the topography) and the highest values in July and August (values between 3,000 and 4,000 m asl). The southern Swiss winter ZDL is up to 500 m higher than the one in northern Switzerland. The differences become smaller in spring and autumn and very similar ZDL values are found in summer. The ZDL's year-to-year variability is very large in winter with a range of almost 3,000 m and is substantially smaller in spring and summer (range mostly about 1,000 m). The mean and median values of the most recent period are on average several 100 m higher than those of the pre-industrial time. More details on the ZDL evolution and variability differences in the period 1864–2019 are discussed in Section 4.2.

4.2 | Evolution and trends

Figure 8 shows the long-term evolution of the northern and southern Swiss ZDL from 1864 to 2019. The values of the individual months (points in Figure 8) again highlight the large interannual variability of the ZDL values in the winter months (Figure 8a,b) compared to the other seasons, especially the summer months (Figure 8e,f). The variabilities are somewhat larger in northern Switzerland than in southern Switzerland, again especially in winter months. The time series show increases in all months. However, the 30-year running mean curves display considerable decadal variability and differences between the months and seasons. The evolution of the three winter

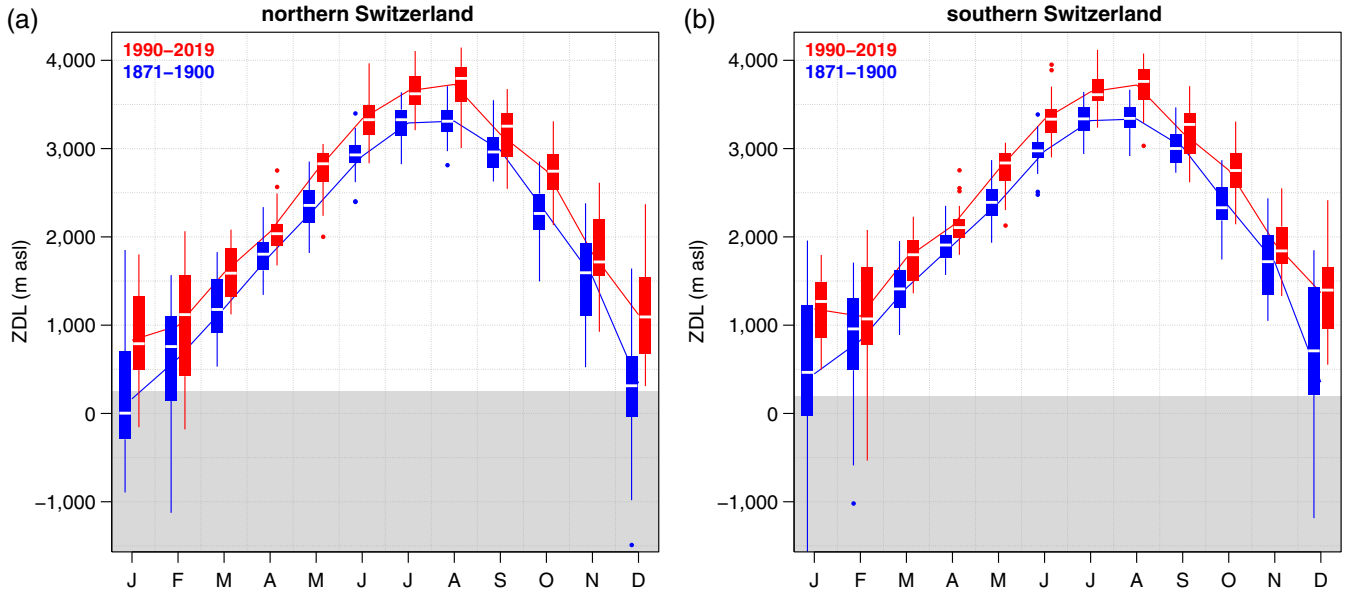

FIGURE 7 Annual cycle of the ZDL in northern Switzerland (Panel a, left) and in southern Switzerland (Panel b, right) for the two 30-year periods 1871–1900 (blue) and the current period 1990-2019 (red). The solid lines connecting the months show the mean estimates. The boxplots show the median (white line), the 25th–75th percentile range, the whiskers (max(ZDL_{min}; $ZDL_{q25\ -\ 1.5 \cdot IQR}$) to min($ZDL_{max}$; $ZDL_{q75\ +\ 1.5 \cdot IQR}$)), dots represent values outside the whiskers (outliers). Elevations below the lowest point of the topography are shaded in grey. Note that, the mean ZDL is significantly higher 1990–2019 than 1871–1900 in all 12 months ($p < 0.05$) [Colour figure can be viewed at wileyonlinelibrary.com]

months is very different with a small and relatively steady increase in February but large and unsteady increases in December and January. The evolution in the summer months is very similar with most of the increases taking place since the 1980s. Also in the three spring months, the evolution is similar with a somewhat smaller increase in April. In autumn, September and November evolve similarly and relatively slowly, while a large and very steady increase is obtained in October. The differences between northern and southern Switzerland are relatively small. Only in the winter months, the evolution differs considerably.

Figure 9 shows two estimates for the long-term ZDL changes in northern and southern Switzerland. In both regions, the ZDL has significantly increased in all 12 months. This is true for the changes in the 30-year means (95% Student-*t* confidence interval [CI] is positive for all months) as well as the change estimate using the Theil–Sen (TS) trend multiplied with a comparable period length (Mann–Kendall trend test $p < 0.05$ for all months). For northern Switzerland (Figure 9a), the largest ZDL increases are found for December and January with mean values of about 700 and 600 m, respectively. However, the values are subject to very large uncertainties (95% CI: ±400 m). The smallest increases are found for April and September with 200–250 m. For most other months (except October with almost 500 m), the increase is 300–400 m. The TS change estimate is systematically lower than the mean change estimate in spring and summer and similar in autumn and winter. However, the mean change 95% CI includes the TS change in all months. The differences might indicate that a linear model is not ideal to describe the ZDL changes in spring and summer, where temperature has not increased for a long time but rapid increases have been observed in the recent decades (Figure 8). For southern Switzerland (Figure 9b), the long-term ZDL increases tend to be somewhat smaller than those in northern Switzerland but otherwise show similar month-to-month changes.

Table 1 lists 1871–2019 long-term and 1970–2019 near-term TS-trends and the total ZDL change differences between northern and southern Switzerland for the two trend periods. The change results from Figure 9 are confirmed. In all months, the northern Swiss long-term trends (range: 19.3–55.5 m·decade^{-1}) are larger than the southern Swiss trends (range: 16.0–37.1 m·decade^{-1}). The ZDL change differences are about 100–400 m in winter months and smaller than 100 m in the other seasons. In the near-term (1970–2019), the ZDL trends are significant from March to August (plus October for northern Switzerland) showing very large increases between 58.9 and 139.5 m·decade^{-1}. The TS trend values for September and November to February are positive (28.8–70.0 m·decade^{-1}) but not significant ($p > 0.05$). The

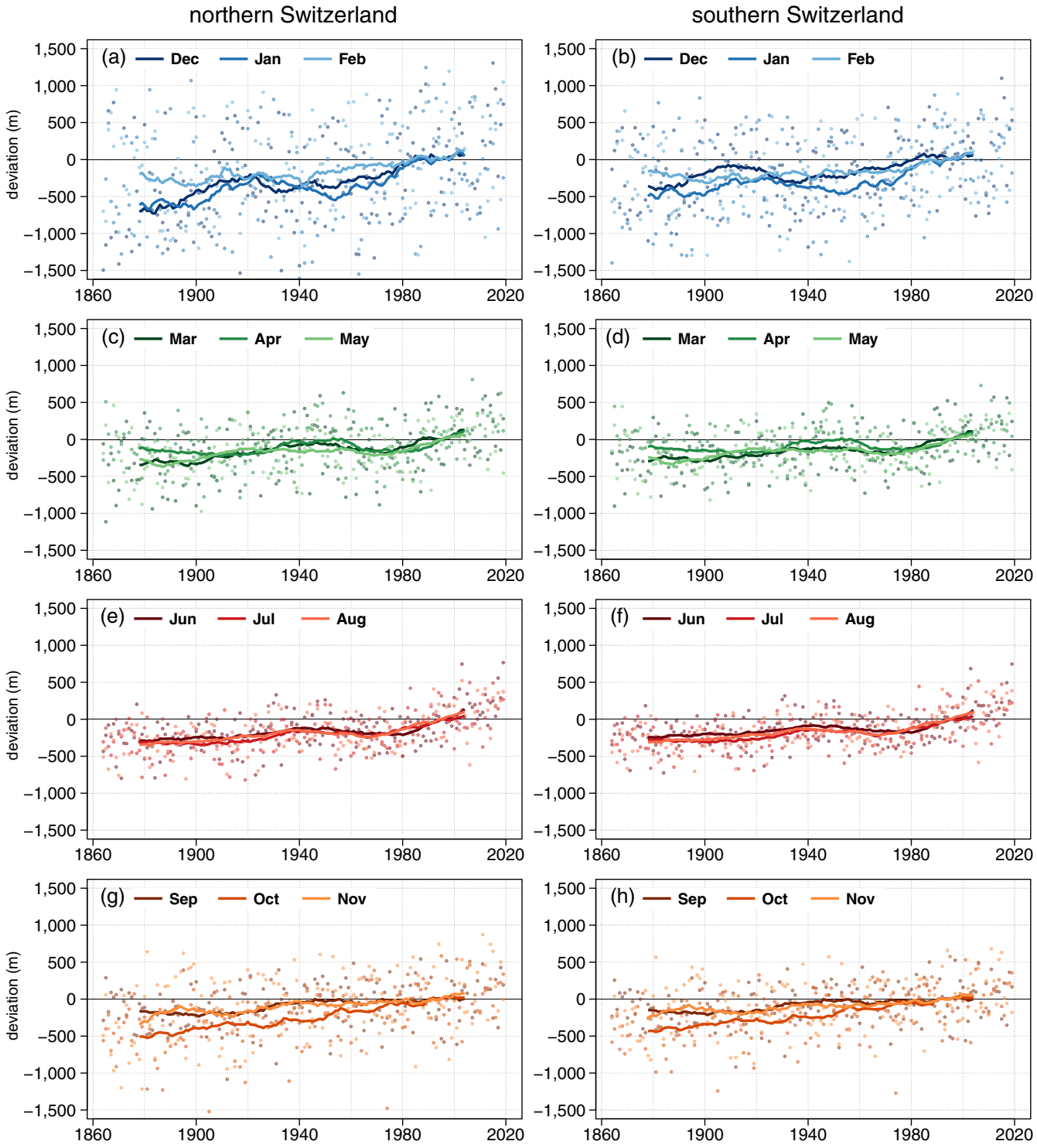

FIGURE 8 ZDL evolution in the period 1864–2019 shown as deviation from the 1981–2010 monthly mean for northern Switzerland (left Panels a,c,e and g) and for southern Switzerland (right Panels b,d,f and h). Panels a,b: winter months December, January and February. Panels c, d: spring months March, April and May. Panels e, f: summer months June, July and August. Panels g, h: Autumn months September, October and November. The monthly values are shown as dots, the solid lines show centred 30-year running mean values. Colours are explained in the legend. Units shown are metres. For better visibility, 11 strongly negative winter ZDL deviations between −1,632 and −2,550 m have been cropped [Colour figure can be viewed at wileyonlinelibrary.com]

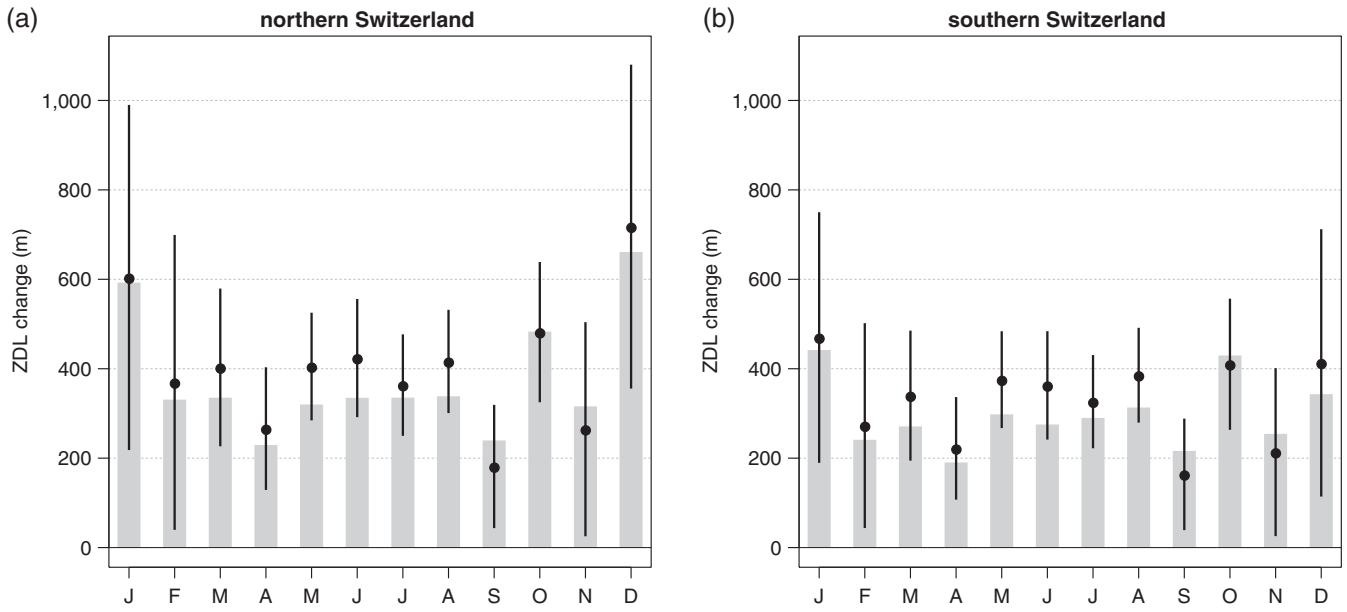

FIGURE 9 Long-term monthly ZDL change estimates in metres for northern Switzerland (Panel a, left) and southern Switzerland (Panel b, right). Shown are the differences of the means of the period 1990–2019 and the pre-industrial period 1871–1900 (change estimate 1: dots depict the mean estimate; the vertical line segments show the 95% Student-*t* confidence interval) and the change given by the 1871–2019 Theil–Sen trend estimate multiplied with a period length of 119 years, the difference of the central years 1885 and 2004 of the periods used for change estimate 1 (change estimate 2: grey bars)

TABLE 1 Monthly long-term (1871–2019) and near-term (1970–2019) Theil–Sen trend estimates for northern (m_N) and southern (m_S) Switzerland (units: m·decade^{-1})

	Jan	Feb	Mar	Apr	May	Jun	Jul	Aug	Sep	Oct	Nov	Dec
Long-term: 1871–2019												
m_N	49.8	27.8	28.2	19.3	26.9	28.1	28.2	28.4	20.1	40.6	26.5	55.5
m_S	37.1	20.3	22.8	16.0	25.0	23.1	24.4	26.3	18.2	36.1	21.4	28.8
d_{N-S}	**189**	**113**	80	49	28	75	57	31	29	67	77	**398**
Near-term: 1970–2019												
m_N	52.1*	41.0*	84.1	139.5	70.7	134.0	92.9	102.8	28.8*	58.9	62.5*	70.0*
m_S	35.0*	52.8*	87.1	108.3	74.0	113.6	88.7	100.1	27.8*	54.7*	38.9*	30.7*
d_{N-S}	89	−59	−15	**156**	−16	**102**	21	14	5	21	**118**	**197**

Note: d_{N-S} show the ZDL change difference between northern and southern Switzerland (long-term: $(m_N - m_S)$·14.9 decades, short-term: $(m_N - m_S)$·five decades, units: m). Differences >100 m are in bold and all values are rounded to full metres. Trends not significant (Mann–Kendall trend test $p > 0.05$) are shown with an asterisk.

trends are similar for both regions with a small tendency for somewhat larger trends in northern Switzerland in most months.

4.3 | Current scaling with temperature

Scaling quantities with temperature is an easily understandable and often used concept in applied environmental research. It has for example been applied for changes in FL (Diaz *et al.*, 2003) or the snowline (Hantel *et al.*, 2012). In Figure 10 we show estimates of the annual cycle of the current (1970–2019) ZDL-temperature scaling, that is, the linear regression of monthly ZDL with Swiss mean temperature in m·°C^{-1}. The ZDL-temperature scalings are all highly significant and show a pronounced seasonal cycle. For northern Switzerland, the scalings range from +150–170 m·°C^{-1} (April–August) up to +340 m·°C^{-1} (December). The uncertainties are again highest in December and January (95% Student-*t* CI: ±45 m·°C^{-1}) and relatively small in spring and summer (95% CI: <±10 m·°C^{-1}). For southern

Switzerland, the scalings are somewhat smaller from November to March with a maximum of about 265 ± 20 m·°C^{-1} in December and January. For both regions, the summer-half year values are relatively close to the inverse of the environmental lapse rate of 6.5°C km^{-1} (154 m·°C^{-1}).

4.4 | Discussion

The results presented above indicate a number of interesting features in the ZDL variability. For instance, the interannual winter variability of the ZDL values expressed as standard deviation is about a factor 2–2.5 times the summer variability. This is substantially higher than the ratio of winter and summer temperature variability, which is only ~1.3–1.7 using northern Swiss monthly mean temperature series. We hypothesize that the large difference is mainly caused by the strong profile non-linearities, which additionally enlarge the range of ZDL values and thus winter ZDL variability. The winter ZDL variabilities are about 30–40% larger in northern Switzerland than in southern Switzerland. It seems that the largest part of these differences is caused by the 20–30% larger northern Swiss temperature variabilities.

On a multi-decadal time scale, the analysis of the ZDL evolution has shown significant increases ($p < 0.05$) for all months with minor differences between northern and southern Switzerland. The largest differences are found in winter, where the northern Swiss trends and temperature scalings are larger than in southern Switzerland. This is very similar to the temperature evolution, which also differs most in winter months. In the last 150 years, low elevation winter temperature has increased by about 2.4°C in northern Switzerland but by only about 1.5°C in southern Switzerland (Begert and Frei, 2018; Isotta *et al*., 2019). The reasons for these differences are still largely unknown. In the last 50 years (1970–2019), significant ZDL increases have been found in all spring and summer months, while from September to February (except October in northern Switzerland), the trend values are positive but not statistically significant. This is in agreement with recent results on temperature trends in the Swiss Alps. The strong spring and summer warming in recent decades has been shown to be connected to a strong increase of sunshine duration and hence incoming solar radiation in the last four decades (Rottler *et al*., 2019). Winter temperature trends in the last three decades have been strongly modulated by large natural variability, partly masking the effect of global warming (Saffioti *et al*., 2016; Sippel *et al*., 2020; Scherrer, 2020). The somewhat larger trends in northern Switzerland in most months have not been addressed in detail yet. One possible cause could be natural variability, that is, the different influence of weather types north and south of the Alpine ridge.

How do our ZDL trend magnitudes relate to those found in other studies? To compare the obtained long-term trends with other mountain regions is difficult since long-term data is not available for most regions. There

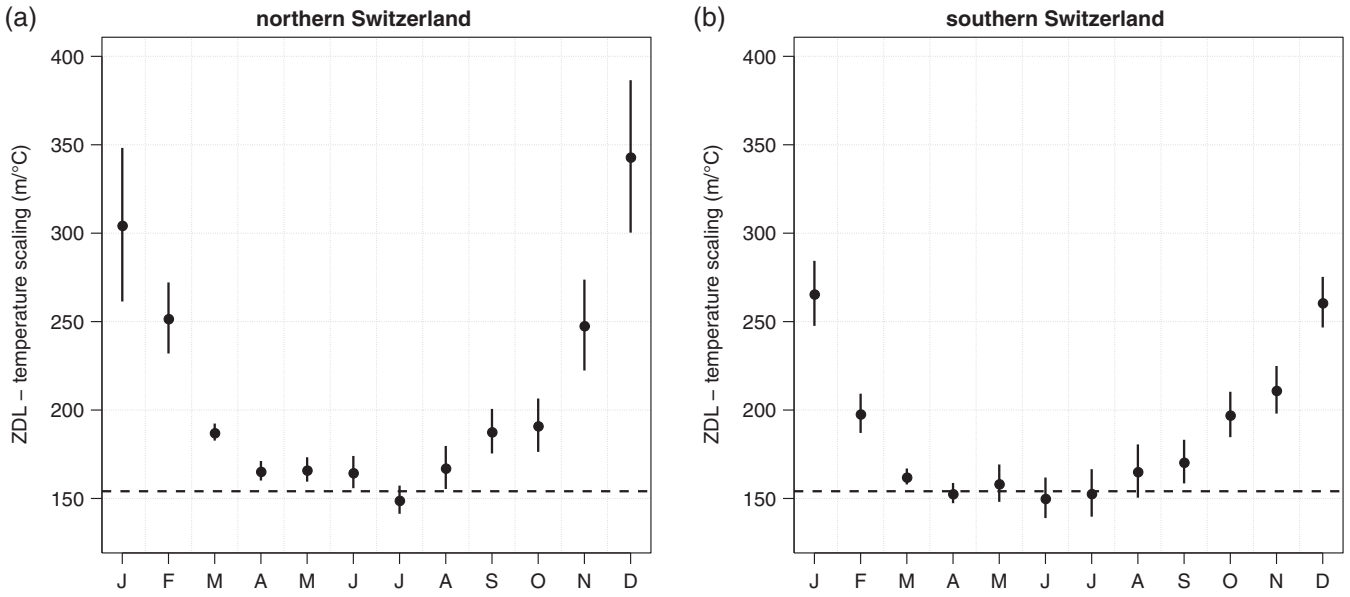

FIGURE 10 ZDL-temperature scaling in m·°C^{-1} for northern Switzerland (Panel a, left) and southern Switzerland (Panel b, right) in the recent period 1970–2019 based on a regression of the monthly ZDL with monthly Swiss mean temperature. Dots: mean estimates, vertical bars: 95% Student-*t* confidence interval. Dashed line: inverse of the environmental lapse rate of 6.5°C km^{-1}

are some large-scale trend studies for shorter time periods, mainly using the free air FL data. For example, Bradley *et al*. (2009) report maximum increases of the annual mean FL between about 25°S and 25°N of about 50–60 m·decade^{-1} in the period 1977–2007. Their region does not cover the European Alps and a direct comparison is thus not possible, but their numbers are smaller than the Swiss ZDL trends (75–85 m·decade^{-1}) for the same period. Part of the difference might be explained by the fact that free air data is compared with the near-surface ZDL (Section 3.3), but at the moment, an exact quantification is impossible.

Related to the ZDL evolution, but not identical with it, is the evolution of the Alpine snowline. Hantel *et al*. (2012) found that the median Alpine snowline in the 1961–2010 period increased by 166 m·°C^{-1} in winter and about 123 m·°C^{-1} in summer. Our ZDL-temperature scalings are roughly twice as large in winter (250–350 m·°C^{-1}) and somewhat larger in summer (∼160 m·°C^{-1}). Hu *et al*. (2020) analysed changes in the snowline during the ablation season from April to June for large catchments in the Alps using satellite data for the period 1984–2018. They found increasing snowline trends of about 52 ± 28 m·decade^{-1} (90% CI) for the northern Alpine Alpenrhein catchment and very similar values for the southern Alpine Adda catchment (50 ± 31 m·decade^{-1}). Our ZDL trends in the same time period are more than twice as large (133 ± 40 m·decade^{-1} (90% CI) for northern Switzerland; 118 ± 37 m·decade^{-1} for southern Switzerland). Not astonishingly, this short comparison shows that the ZDL and snowline trends are related, but that the ZDL reacts more strongly to temperature changes than the snowline. A more quantitative analysis would certainly be interesting but is beyond the scope of this article.

5 | SENSITIVITIES IN A WARMING CLIMATE

To assess the influence of the non-linear nature of the northern and southern Swiss temperature profiles upon the ZDL evolution in a strongly warming climate, we apply a wide range of possible temperature changes onto the monthly *inv_type* profiles of the 1981–2010 normal period (Figure 3c,d). The T–z profile is described by five parameters (cf., Section 2.3.2), which in principle also would allow to mimic specific and potentially interesting changes such as elevation dependent warming (MRI EDW Working Group, 2015; Rangwala and Miller, 2012) or changes of the inversion characteristics. To keep things simple, and since there are no clear signs for robust changes of the parameters apart from the changes in mean temperature in the past evolution (Figure S4), we restrict our analysis to an elevation-independent temperature shift dT of the monthly mean 1981–2010 temperature profiles by −2 to +5°C. The −2°C roughly corresponds to pre-industrial levels, the +5°C is roughly the mean change signal of a high emission scenario (RCP8.5) at the end of the 21st century (CH2018, 2018).

Figure 11a,b shows the monthly ZDL elevation as a function of dT. From March to October, the ZDL increases more or less linearly over the whole dT range. Non-linearities are found from November to February. They are limited to certain dT values which depend on the region. For northern Switzerland, the ZDL increases are stronger mainly for dT values between −1°C (near past) and +2°C for DJF and negative dT (past) for November. For southern Switzerland, the non-linearities are mostly smaller and strongest for negative dT values. The stronger ZDL increases in winter bring the winter, spring and autumn values closer together for large dTs. For example, the northern Swiss December ZDL becomes similar to the March ZDL for large dT values while having been about 800 m below the March ZDL for dT = −2°C (roughly the pre-industrial level). Another example is the November ZDL which transitions to March for dT = −2°C and moves up to the April ZDL for dT = +5°C.

Figure 11c,d shows the ZDL change ($dZDL$) as a function of dT. For negative dT values, stronger ZDL increases are found from November to February compared to the other months. Assuming an elevation-independent warming of 2°C and the ZDL-temperature scaling from Figure 10a, the northern Swiss ZDL change from November to February should be about 500–800 m, while only 320–340 m for the other months. This agrees well with the higher trends found for the winter months compared to the summer months in the historical analysis (Figures 8, 9). Differences in individual months can be well explained since the 1871–2019 warming trends show a substantial range of about +1–3°C. A similar pattern is found for positive dT values. The total winter ZDL increases assuming a strong temperature shift (dT = 5°C) are considerably larger (northern Switzerland: +1,250–1,600 m and southern Switzerland: +1,000–1,150 m) than those in the other months (+800–1,000 m).

Figure 11e,f shows the ZDL-temperature scaling ($dZDL/dT$) as a function of dT. From March to October, scalings are about 160(145)–180 m·°C^{-1} in northern (southern) Switzerland and almost independent of dT. Higher and dT-varying ZDL-temperature scalings are mainly found from December to February. For northern

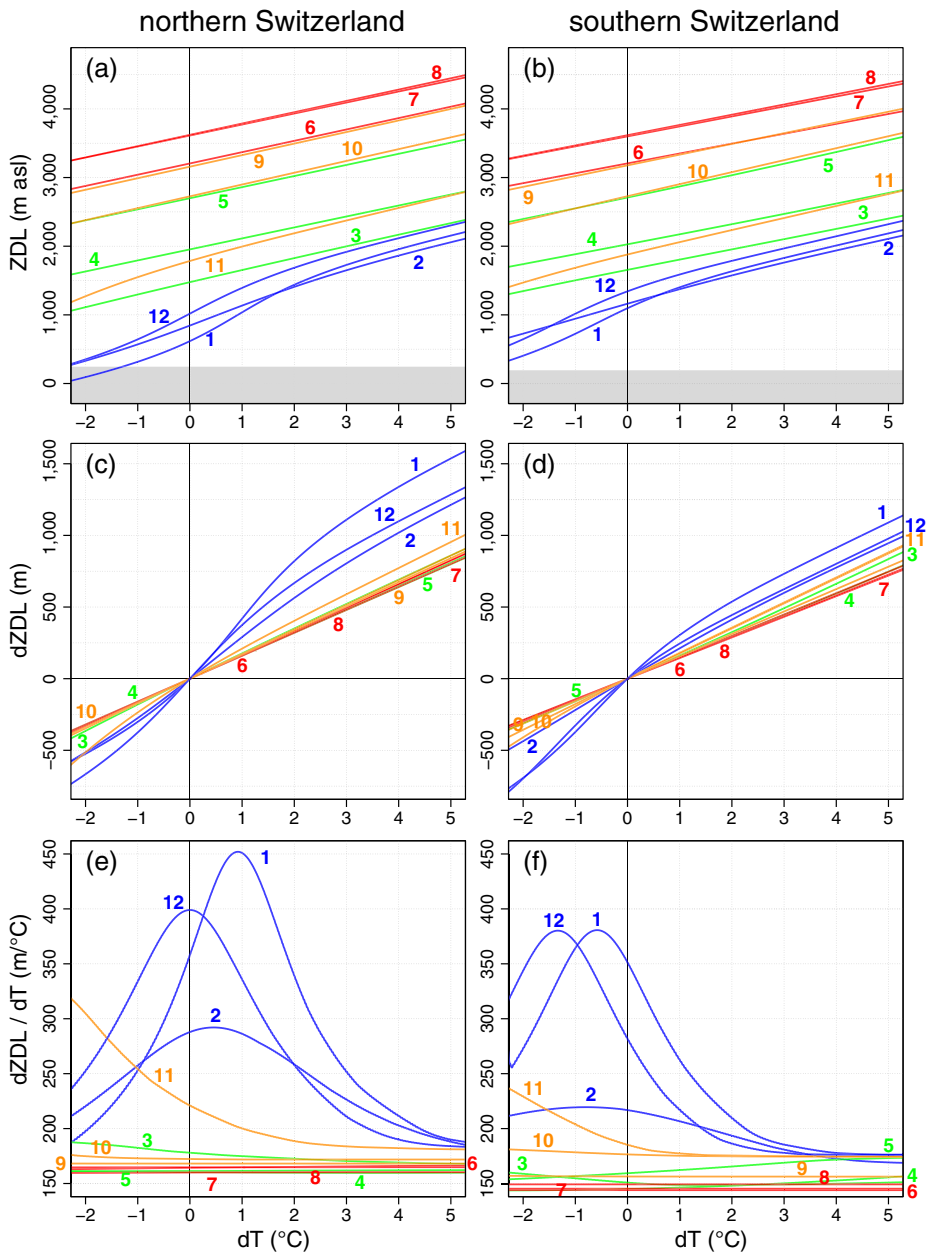

FIGURE 11 Sensitivity of the monthly ZDL as function of a warming dT. Panels a, c, e: northern Switzerland, Panels b, d, f: Southern Switzerland. Panels a, b: ZDL (m asl). Panels c, d: change of ZDL ($dZDL$) (m asl) with respect to the baseline ZDL for $dT = 0°C$. Panels e, f: ZDL-temperature scaling ($dZDL/dT$) ($m \cdot °C^{-1}$). The months are labelled (1: Jan, 2: Feb, ..., 12: Dec). Winter months are shown in blue, spring months in green, summer months in red and autumn months in orange. Baseline profile temperature ($dT = 0°C$) is the 1981–2010 mean, that is, the ZDLs in panels a,b at $dT = 0°C$ are the same as in Figure 3c,d [Colour figure can be viewed at wileyonlinelibrary.com]

Switzerland (Figure 11e), maximum rates between 300 and 450 $m \cdot °C^{-1}$ are found for dT values around 0°C (today) or +1°C. The values gradually level off to values below 200 $m \cdot °C^{-1}$ for strongly negative and strongly positive dTs. The November values are also higher than those of the non-winter months (~220 $m \cdot °C^{-1}$; $dT = 0°C$). They are even larger for dT <0°C and level off for dT >0°C. For southern Switzerland (Figure 11f), maximum rates of about 375 $m \cdot °C^{-1}$ are found in December and January for dT values between −2 and 0°C (recent past). The values strongly level off to values below 200 $m \cdot °C^{-1}$ for dTs between 0°C (today) and +2°C. The November scalings are somewhat higher (>200 $m \cdot °C^{-1}$) for negative dT values (past), the February scalings for dT values between about −2 (past) and +2°C.

6 | BEST PRACTISES WORLDWIDE

The above results for Switzerland help to give some best practise advice for the ZDL determination in monthly or higher temporal resolution in any mountain area worldwide. The methods presented rely on high data availability as well as on some methodological requirements, but the most important criteria are the regional topographical and meteorological conditions. Figure 12 shows a generic ZDL determination scheme and the main requirements and properties of the recommended methods. The key questions to be answered are:

1. Is the expected ZDL sometimes outside the elevation range of the available data?

2. Are there important non-linearities in the T–z profile?

If the answer to Question 1 is an unconditional NO, that is, if no extrapolation is necessary at all times, the intuitive and purely data driven *near 0°C* method is the most obvious option to choose, although the *linear* fit and *non-linear* fit could also be checked for suitability. The *near 0°C* method, however, only works if enough data around 0°C is available. It also requires a subjective definition of a temperature range around 0°C to be sampled for averaging and, in principle, allows for deriving several ZDLs.

If the answer to Question 1 is YES, a parametric function should be fitted to the T–z data, and Question 2 helps to determine which one. Note that the answer to Question 2 is not straightforward in most cases and an in-depth analysis of the effects of different profile models is necessary. Also for the Swiss Alps, a thorough validation was necessary (Section 3) before this question could be answered. If the answer to Question 2 is NO, the linear fit is the method of choice. The data requirements are quite small ($n \geq 5$ recommended, Lute and Abatzoglou, 2021) but the data points should cover a large elevation range to ensure a robust fit. Very locally influenced data points should be omitted and a weighting based on geographical location (Frei, 2014) or inclusion of longitude and latitude as covariates in the profile estimation procedure (Li *et al.*, 2013) should be considered. The linear fit is easily applicable to other isotherms since it defines the whole profile in one step but it allows for only one ZDL. If the answer to Question 2 is YES, a non-linear fit should be applied. The data amount required for a non-linear fit is relatively large but difficult to pin down exactly. Our analyses for the southern slope of the Alps show that a non-linear fit with five parameters works well in most cases with 14 data points that cover large parts of the ZDL elevation range. A fitting with a sample size of about 50 is probably on the safe side. The parameter estimation of the non-linear fit is more complex than in the linear case but it allows to determine several ZDLs. Apart from these points, the additional comments made for the linear fit apply also for the non-linear fit (cf., Figure 12).

In this study with Switzerland as testbed, we used the highest ZDL in cases with multiple ZDLs. This choice was of minor importance, as cases with multiple ZDLs were rare. Another choice (e.g., lowest, middle or mean ZDL) might make sense and should be considered depending on the specific application and situation.

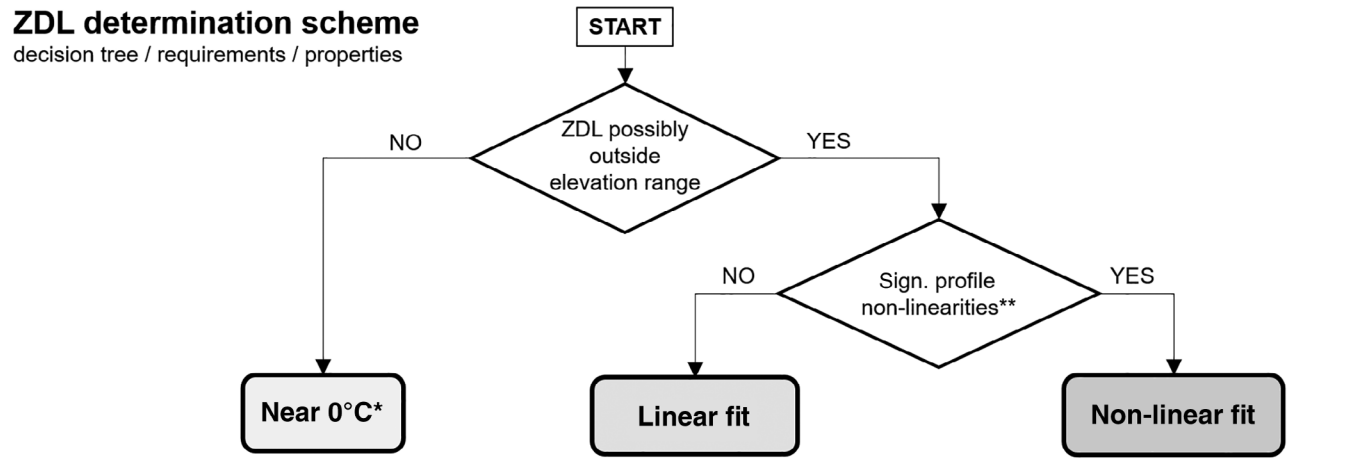

Requirements	*Data*	Data around 0°C needed	Little data needed data covers large elevation range n ≥ 5 recommended	Considerable data needed data covers large elevation range Alps: $n \geq 14$ works in most cases
	Method	Subjective constants definition	Station pre-selection / weighting	
			Simple parameter estimation	Complex parameter estimation
Further properties		Purely data driven (non-param.)	Defines whole profile, easy application to other isotherms	
		Allows several ZDL	Allows only one ZDL	Allows up to three ZDL

** check also linear and non-linear fit if data permits*
*** extensive investigations might be necessary to decide this*

FIGURE 12 Near-surface ZDL determination scheme for an arbitrary mountain region. The upper part presents a decision tree with questions on the climatological and topographical conditions in the region as a supporting tool for specific method-selection (boxes with bold borders). The lower part lists important data and methodological requirements and some further properties of the three methods

7 | CONCLUSIONS

The ZDL is a key isotherm for hydrology, glaciology and ecology in mountain regions worldwide and can serve as a key indicator of climate change. However, there is a lack of knowledge about ZDL estimation methodologies and their properties. One aim of this study was to close some of these gaps. To this end, we tested different approaches to determine the near-surface ZDL for climatological purposes on a monthly time scale. As testbed, the northern and southern slopes of the Swiss Alps have been chosen. We found that a non-linear profile method delivered more robust and more realistic ZDL estimates than a linear profile method especially in winter but also throughout the year. It should however be noted, that the concept of a winter ZDL on the monthly scale can have a limited applicability and caution is needed when using monthly mean data to determine a monthly ZDL, also if a non-linear approach is used.

In the last 150 years, the Swiss Alpine ZDL has significantly increased in all months. The ZDL increases in northern Switzerland are mostly around 300–400 m (TS-trend: ~26–28 m·decade^{-1}) with smaller values in April and September (200–250 m, TS-trend: ~20 m·decade^{-1}) and a larger value in October (almost 500 m, TS-trend: 41 m·decade^{-1}). The largest increases but also the largest uncertainties are found in December and January (600–700 ± 400 m; TS-trend: ~50 ± 30 m·decade^{-1}, 95% confidence interval). Southern Swiss trends are somewhat smaller, especially in winter months. On both sides of the Alps, the positive ZDL trends have accelerated in the last five decades especially in spring and summer with increases between 70 and 140 m·decade^{-1}. Recent ZDL-temperature scalings vary considerably throughout the year. Low values between 150 and 170 m·°C^{-1}, close to the inverse of the environmental lapse rate, are found in the summer-half year. In winter, linked to the impact of inversions, values up to 340 ± 45 m·°C^{-1} are found for northern Switzerland and up to 270 ± 20 m·°C^{-1} in southern Switzerland. A comparison of the ZDL and the Alpine snowline indicates that the recent trends and temperature-scalings of the ZDL are considerably larger than those of the snowline.

The ZDL-temperature scalings strongly depend on the climate state and in a changing climate also on time. Our analysis shows that the winter scalings are probably near a maximum today or in the near future and that the scaling values are expected to decrease towards the summer values under a strong future warming. However, the cumulative ZDL increase assuming a strong warming would still be considerably larger in winter than in summer. A simple linear lapse rate approach is not able to represent the changing ZDL-temperature scalings. This is particularly relevant in the Alps with their pronounced profile non-linearities and aggravates for long-term analyses and climate change scenarios with temperature changes of several degrees Celsius.

Finally, we presented best practises for the ZDL determination in other mountain regions based on two key criteria: data availability for different elevations and the importance of profile non-linearities. The method requirements and other key properties have also been discussed. The parametric methods outlined could be easily extended to other important isotherms or the assessment of the whole temperature profile. The analysis lays the foundation to study the ZDL in future climate projections using climate scenario data.

ACKNOWLEDGEMENTS

The authors thank Francesco Isotta for producing additional data and Christoph Frei and Flavian Tschurr (all MeteoSwiss) and two anonymous reviewers for their valuable input.

AUTHOR CONTRIBUTIONS

Simon Scherrer: Conceptualization; formal analysis; investigation; methodology; visualization; writing-original draft; writing-review & editing. **Stefanie Gubler:** Conceptualization; investigation; methodology; visualization; writing-original draft; writing-review & editing. **Kathrin Wehrli:** Conceptualization; methodology; writing-original draft; writing-review & editing. **Andreas Fischer:** Conceptualization; methodology; writing-original draft; writing-review & editing. **Sven Kotlarski:** Conceptualization; methodology; supervision; writing-original draft; writing-review & editing.

ORCID

Simon C. Scherrer https://orcid.org/0000-0002-5040-0470
Stefanie Gubler https://orcid.org/0000-0002-3733-953X
Kathrin Wehrli https://orcid.org/0000-0001-7692-6676
Andreas M. Fischer https://orcid.org/0000-0003-0832-3675
Sven Kotlarski https://orcid.org/0000-0001-9542-6781

REFERENCES

Beniston, M. (2014) European isotherms move northwards by up to 15 km year^{-1}: using climate analogues for awareness-raising. *International Journal of Climatology*, 34, 1838–1844. https://doi.org/10.1002/joc.3804.

Begert, M., Frei, C. (2018) Long-term area-mean temperature series for Switzerland - Combining homogenized station data and high resultion grid data. *International Journal of Climatology*, 38, 2792–2807, https://doi.org/10.1002/joc.5460

Blandford, T.R., Humes, K.S., Harshburger, B.J., Moore, B.C., Walden, V.P. and Ye, H. (2008) Seasonal and synoptic variations in near-surface air temperature lapse rates in a Mountainous

Basin. *The Journal of Applied Meteorology and Climatology*, 47, 249–261. https://doi.org/10.1175/2007JAMC1565.1.

Bony, S., Colman, R., Kattsov, V.M., Allan, R.P., Bretherton, C.S., Dufresne, J.-L., Hall, A., Hallegatte, S., Holland, M.M., Ingram, W., Randall, D.A., Soden, D.J., Tselioudis, G. and Webb, M.J. (2006) How well do we understand and evaluate climate change feedback processes? J. *Climate*, 19, 3445–3482. https://doi.org/10.1175/JCLI3819.1.

Bradley, R.S., Keimig, F.T., Diaz, H.F. and Hardy, D.R. (2009) Recent changes in freezing level heights in the tropics with implications for the deglacierization of high mountain regions. *Geophysical Research Letters*, 36, L17701. https://doi.org/10.1029/2009GL037712.

Brocard, E., Jeannet, P., Begert, M., Levrat, G., Philipona, R., Romanens, G. and Scherrer, S.C. (2013) Upper air temperature trends above Switzerland 1959–2011. *Journal of Geophysical Research – Atmospheres*, 118, 4303–4317. https://doi.org/10.1002/jgrd.50438.

Brogli, R., Kröner, N., Sorland, S., Lüthi, D. and Schär, C. (2019) The role of Hadley circulation and lapse-rate changes for the future European summer climate. *Journal of Climate*, 32, 385–404. https://doi.org/10.1175/JCLI-D-18-0431.1.

Carrasco, J.F., Gino, C.G. and Quintana, J. (2005) Changes of the 0°C isotherm and the equilibrium line altitude in Central Chile during the last quarter of the 20th century. *Hydrological Sciences Journal*, 50, 933–948. https://doi.org/10.1623/hysj.2005.50.6.933.

Ceppi, P., Scherrer, S.C., Fischer, A.M. and Appenzeller, C. (2012) Revisiting Swiss temperature trends 1959–2008. *International Journal of Climatology*, 32, 203–213. https://doi.org/10.1002/joc.2260.

CH2018. (2018). *CH2018. – Climate Scenarios for Switzerland, Technical Report*. National Centre for Climate Services, Zurich. Available at: https://www.klimaszenarien.ch.

Cleveland, W.S., Grosse, E. and Shyu, W.M. (1992) Local regression models. In: Chambers, J.M. and Hastie, T.J. (Eds.) *Statistical Models*. Boca Raton: Wadsworth & Brooks/Cole. https://doi.org/10.1201/9780203738535.

Diaz, H.F., Eischeid, J.K., Duncan, C. and Bradley, R.S. (2003) Variability of freezing levels, melting season indicators, and snow cover for selected high-elevation and continental regions in the last 50 years. *Climatic Change*, 59, 33–52. https://doi.org/10.1023/A:1024460010140.

Diaz, H.F. and Graham, N.E. (1996) Recent changes in tropical freezing heights and the role of sea surface temperature. *Nature*, 383, 152–155. https://doi.org/10.1038/383152a0.

Dutra, E., Muñoz Sabater, J., Boussetta, S., Komori, T., Hirahara, S. and Balsamo, G. (2020) Environmental lapse rate for high-resolution land surface downscaling: an application to ERA5. *Earth and Space Science*, 7, e2019EA000984. https://doi.org/10.1029/2019EA000984.

Frei, C. (2014) Interpolation of temperature in a mountainous region using non-linear profiles and non-Euclidean distances. *International Journal of Climatology*, 34, 1585–1605. https://doi.org/10.1002/joc.3786.

Güller A. (1979) Die Nullgradgrenze in der Schweiz 1951–1978 nach den Radiosondierungen von Payerne, in Klimatologie der Schweiz, Band 21, Beiheft zu den Annalen der Schweizerischen Meteorologischen Zentralanstalt, Zürich, 56p, (in German).

Hantel, M., Maurer, C. and Mayer, D. (2012) The snowline climate of the Alps 1961-2010. *Theoretical and Applied Climatology*, 110, 517–537. https://doi.org/10.1007/s00704-012-0688-9.

Hiebl, J. and Schöner, W. (2018) Temperature inversions in Austria in a warming climate - changes in space and time, 27, 309–323. https://doi.org/10.1127/metz/2018/0899.

Hock, R. and Rasul, G. (2019). *High mountain areas (Chapter 2)*. IPCC Special Report on the Ocean and Cryosphere in a Changing Climate (Available at: https://www.ipcc.ch/srocc/chapter/chapter-2/).

Hu, Z., Dietz, A., Zhao, A., Uereyen, S., Zhang, H., Wang, M., Mederer, P. and Kuenzer, C. (2020) Snow moving to higher elevations: analyzing three decades of snowline dynamics in the Alps. *Geophysical Research Letters*, 47, e2019GL085742. https://doi.org/10.1029/2019GL085742.

Hüsler, F., Jonas, T., Riffler, M., Musial, J.P. and Wunderle, S. (2014) A satellite-based snow cover climatology (1985–2011) for the European Alps derived from AVHRR data. *The Cryosphere*, 8, 73–90. https://doi.org/10.5194/tc-8-73-2014.

Ibañez, M., Gironás, J., Oberli, C., Chadwick, C., & Garreaud, R.D. (2020). Daily and seasonal variation of the surface temperature lapse rate and 0°C isotherm height in the western subtropical Andes. https://doi.org/10.1002/joc.6743

Immerzeel, W.W., Petersen, L., Ragettli, S. and Pellicciotti, F. (2014) The importance of observed gradients of air temperature and precipitation for modeling runoff from a glacierized watershed in the Nepalese Himalayas. *Water Resources Research*, 50, 2212–2226. https://doi.org/10.1002/2013WR014506.

Isotta, F.A., Begert, M. and Frei, C. (2019) Long-term consistent monthly temperature and precipitation grid data sets for Switzerland over the past 150 years. *Journal of Geophysical Research: Atmospheres*, 124, 3783–3799. https://doi.org/10.1029/2018JD029910.

Kattel, D.B., Yao, T., Yang, K., Tian, L., Yang, G. and Joswiak, D. (2013) Temperature lapse rate in complex mountain terrain on the southern slope of the central Himalayas. *Theoretical and Applied Climatology*, 113, 671–682. https://doi.org/10.1007/s00704-012-0816-6.

Kirchner, M., Theresa, F.-K., Gert, J., Michael, L., Ludwig, R., Hans-Eckhart, S. and Peter, S. (2013) Altitudinal temperature lapse rates in an Alpine valley: trends and the influence of season and weather patterns. *International Journal of Climatology*, 33(3), 539–555. https://doi.org/10.1002/joc.3444.

Korolev, A., McFarquhar, G., Field, P.R., Franklin, C., Lawson, P., Wang, Z., Williams, E., Abel, S.J., Axisa, D., Borrmann, S., Crosier, J., Fugal, J., Krämer, M., Lohmann, U., Schlenczek, O., Schnaiter, M., Wendisch, M. (2017) Mixed-phase clouds: progress and challenges. *Meteorological Monographs*, 58, 5.1–5.50. https://doi.org/10.1175/AMSMONOGRAPHS-D-17-0001.1.

Kotlarski, S., Lüthi, D. and Schär, C. (2015) The elevation dependency of 21st century European climate change: an RCM ensemble perspective. *International Journal of Climatology*, 35, 3902–3920. https://doi.org/10.1002/joc.4254.

Kottek, M., Grieser, J., Beck, C., Rudolf, B. and Rubel, F. (2010) World map of the Köppen-Geiger climate classification updated. *Meteorologische Zeitschrift*, 15, 259–263. https://doi.org/10.1127/0941-2948/2006/0130.

Kröner, N., Kotlarski, S., Fischer, E., Lüthi, D., Zubler, E. and Schär, C. (2017) Separating climate change signals into thermodynamic, lapse-rate and circulation effects: theory and application to the European summer climate. *Climate Dynamics*, 48, 3425–3440. https://doi.org/10.1007/s00382-016-3276-3.

Li, X., Wang, L., Chen, D., Yang, K., Xue, B. and Sun, L. (2013) Near-surface air temperature lapse rates in the mainland China during 1962–2011. *Journal of Geophysical Research – Atmospheres*, 118, 7505–7515. https://doi.org/10.1002/jgrd.50553.

Lute, A.C. and Abatzoglou, J.T. (2021) Best practices for estimating near-surface air temperature lapse rates. *International Journal of Climatology*, 41, E110–E125. https://doi.org/10.1002/joc.6668.

Lüthi, S., Ban, N., Kotlarski, S., Steger, C.R., Jonas, T. and Schär, C. (2019) Projections of alpine snow-cover in a high-resolution climate simulation. *Atmosphere*, 10, 463. https://doi.org/10.3390/atmos10080463.

Lynn, E., Cuthbertson, A., He, M., Vasquez, J.P., Anderson, M.L., Coombe, P., Abatzoglou, J.T. and Hatchett, B.J. (2020) Technical note: precipitation-phase partitioning at landscape scales to regional scales. *Hydrology and Earth System Sciences*, 24, 5317–5328. https://doi.org/10.5194/hess-24-5317-2020.

MeteoSchweiz (2019) Klimareport 2018. Bundesamt für Meteorologie und Klimatologie MeteoSchweiz, Zürich. 94. (Available at: German, French and Italian from https://www.meteoswiss.ch

Micu, D.M., Dumitrescu, A., Cheval, S., Nita, I.-A. and Birsan, M.-V. (2020) Temperature changes and elevation-warming relationships in the Carpathian Mountains. *International Journal of Climatology*, 41, 2154–2172. https://doi.org/10.1002/joc.6952.

Minder, J.R., Mote, P.W. and Lundquist, J.D. (2010) Surface temperature lapse rates over complex terrain: lessons from the Cascade Mountains. *Journal of Geophysical Research*, 115, D14122. https://doi.org/10.1029/2009JD013493.

Mountain Research Initiative EDW Working Group. (2015) Elevation-dependent warming in mountain regions of the world. *Nature Climate Change*, 5, 424–430. https://doi.org/10.1038/nclimate2563.

Pepin, N.C. and Seidel, D.J. (2005) A global comparison of surface and free-air temperatures at high elevations. *Journal of Geophysical Research*, 110, D03104. https://doi.org/10.1029/2004JD005047.

Pruppacher, H.R., & Klett, J.D. (2010). *Microphysics of Clouds and Precipitation, Atmospheric and Oceanographic Sciences Library Book Series (ATSL)*, Volume 18, https://doi.org/10.1007/978-0-306-48100-0

Rangwala, I. and Miller, J.R. (2012) Climate change in mountains: a review of elevation-dependent warming and its possible causes. *Climatic Change*, 114, 527–547. https://doi.org/10.1007/s10584-012-0419-3.

Richner, H. and Phillips, P.D. (1984) A comparison of temperatures from mountaintops and the free atmosphere: their diurnal variation and mean difference. *Monthly Weather Review*, 112, 1328–1340. https://doi.org/10.1175/1520-0493(1984)112<1328:ACOTFM>2.0.CO;2.

Rolland, C. (2003) Spatial and seasonal variations of air temperature lapse rates in alpine regions. *Journal of Climate*, 16, 1032–1046. https://doi.org/10.1175/1520-0442(2003)016<1032:SASVOA>2.0.CO;2.

Rubel, F., Brugger, K., Haslinger, K. and Auer, I. (2017) The climate of the European Alps: shift of very high resolution Köppen-Geiger climate zones 1800–2100. *Meteorologische Zeitschrift*, 26, 115–125. https://doi.org/10.1127/metz/2016/0816.

Rottler, E., Kormann, C., Francke, T., and Bronstert, A. (2019) Elevation-dependent warming in the Swiss Alps 1981–2017: Features, forcings and feedbacks, International *Journal of Climatology*, 39, 2556–2568, https://doi.org/10.1002/joc.5970.

Salzmann, N., Scherrer, S.C., Allen, S., Rohrer, M. (2015) Temperature, precipitation and related extremes in mountain areas. In: Huggel, C., et al. (Eds.) *The High-Mountain Cryosphere - Environmental Changes and Human Risks*. Cambridge, UK: Cambridge University Press, pp. 28–49. https://doi.org/10.1017/CBO9781107588653.

Saffioti, C., Fischer, E.M., Scherrer, S.C., and Knutti, R. (2016) Reconciling observed and modeled temperature and precipitation trends over Europe by adjusting for circulation variability, *Geophysical Research Letters*, 43, 8189–8198, https://doi.org/10.1002/2016GL069802

Schär, C., Davies, T.D., Frei, C., Wanner, H., Widmann, M., Wild, M., et al. (1998) Current Alpine climate. In: Cebon, P., Dahinden, U., Davies, H.C., Imboden, D.M. and Jäger, C. (Eds.) *Views from the Alps: Regional Perspectives on Climate Change*. Boston: MIT Press, pp. 21–72.

Schauwecker, S., Rohrer, M., Huggel, C., Endries, J., Montoya, N., Neukom, R., Perry, B., Salzmann, N., Schwarb, M. and Suarez, W. (2017) The freezing level in the tropical Andes, Peru: an indicator for present and future glacier extents. *Journal of Geophysical Research – Atmospheres*, 122, 5172–5189. https://doi.org/10.1002/2016JD025943.

Scherrer, S.C. (2006). *Interannual climate variability in the European and Alpine region*, PhD thesis, ETH Zürich, Nr. 16338, 120p. https://doi.org/10.3929/ethz-a-005133273

Scherrer, S.C. (2020) Temperature monitoring in mountain regions using reanalyses: lessons from the Alps. *Environmental Research Letters*, 15, 044005. https://doi.org/10.1088/1748-9326/ab702d.

Scherrer, S.C. and Appenzeller, C. (2014) Fog and low stratus over the Swiss plateau – a climatological study. *International Journal of Climatology*, 34, 678–686. https://doi.org/10.1002/joc.3714.

Sippel, S., Fischer, E.M., Scherrer, S.C., Meinshausen, N., and Knutti, R. (2020) Late 1980s abrupt cold season temperature change in Europe consistent with circulation variability and long-term warming, *Environ. Res. Lett.*, 15, 094056, https://doi.org/10.1088/1748-9326/ab86f2

Wanner, H. and Kunz, S. (1983) Klimatologie der Nebel- und Kaltluftkörper im Schweizerischen Alpenvorland mit Hilfe von Wettersatellitenbildern. *Archives for Meteorology, Geophysics, and Bioclimatology, Series B*, 33, 31–56. https://doi.org/10.1007/BF02273989.

SUPPORTING INFORMATION

Additional supporting information may be found online in the Supporting Information section at the end of this article.

How to cite this article: Scherrer, S. C., Gubler, S., Wehrli, K., Fischer, A. M., & Kotlarski, S. (2021). The Swiss Alpine zero degree line: Methods, past evolution and sensitivities. *International Journal of Climatology*, 1–20. https://doi.org/10.1002/joc.7228